Int. J. Electrochem. Sci., 6 **(2011)** 5779 - 5791

International Journal of
ELECTROCHEMICAL
SCIENCE
www.electrochemsci.org

Corrosion Inhibition and Adsorption Properties of N-Phenylhydrazine-1,2-Dicarbothioamide on Mild Steel in Hydrochloric Acid

Sudhish Kumar Shukla [1,2,*], *Ashish Kumar Singh* [1,2], *M.A. Quraishi* [1]

[1] Department of Applied Chemistry, Institute of Technology, Banaras Hindu University, Varanasi, 221005 India
[2] Department of Chemistry, School of Mathematical and Physical sciences, North West University (Mafikeng Campus), Private Bag X2046, Mmabatho 2735, South Africa
[*]E-mail: sudhish.shukla@gmail.com

Received: 20 September 2011 / *Accepted:* 14 October 2011 / *Published:* 1 November 2011

Corrosion Inhibition of the mild steel in 1M HCl N-phenylhydrazine-12-dithiocarboamide (PDA) has been investigated using weight-loss, potentiodynamic polarization and electrochemical impedance spectroscopy (EIS) techniques. Inhibition efficiency increases with increase in inhibitor concentration, and solution temperature. Inhibition efficiency decreases with very slow rate with the increase of the immersion time and the acid concentration. The adsorption of PDA on mild steel in hydrochloric acid solution obeys Langmuir's adsorption isotherm model. Potentiodynamic polarization suggests that PDA acts as mixed type inhibitor. Thermodynamic parameters suggest the adsorption is spontaneous and exothermic process. The results obtained from the three methods used are in good agreement.

Keywords: Mild steel, Adsorption, EIS, Weight loss, Polarization, Activation energy

1. INTRODUCTION

Corrosion is a serious engineering problem in this modern era of the technology advancement and which accounts for economic losses and irreversible structural damage. Acidic solutions are widely used in industries but mild steel suffers severe corrosion in acidic environments. Generally, using organic inhibitors to mitigate corrosion of mild steel in acidic medium is one of the most cost-effective methods [1-5]. The research on organic corrosion inhibitors paid attention to the mechanism of adsorption and also to the relationship between inhibitor structures and their adsorption properties. The adsorption of inhibitors takes place through hetero atoms such as nitrogen, oxygen, phosphorus

and sulphur, triple bond or aromatic rings [1-15]. Generally, the tendency to form a stronger coordination bond and, as consequence, inhibition efficiency should increase in order O<N<S<P [16].

In the present study, we use the condensation product of the thiosemicarbazide and phenyl isothiocynate to investigate the inhibition properties on mild steel corrosion in 1M HCl using weight loss, potentiodynamic polarization and electrochemical impedance spectroscopy methods. Weight loss measurements were used to know the effect of time, temperature and concentration of acid solution on the inhibition properties. Adsorption and activation parameters were calculated to establish the kinetic behaviour of the inhibition process.

2. EXPERIMENTAL

2.1. Inhibitor synthesis

The N-phenylhydrazine-1,2-dithiocarboamide (PDA) was synthesized in the laboratory by refluxing thiosemicarbazide and phenyl isothiocynate in water and ethanol in 1:1 ratio reported elsewhere [17]. The name and structural formula of product are given below:

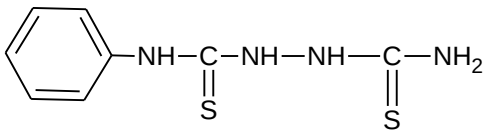

N-phenylhydrazine-1, 2-dicarbothioamide (PDA)

2.2. Corrosion measurements

All the measurements carried out on the mild steel specimens of composition (wt %): C 0.14, Mn 0.035, Si 0.17, S 0.025, P 0.03 and balance Fe. Mild steel specimens were polished prior to all the experiments with emery papers from 600 to 1200 mesh in^{-1}grade. The specimen were washed with double distilled water, degreased with acetone and dried in hot air blower. After drying, the specimen were placed in desiccators and then used for the various experiments. The aggressive solution of 1M HCl was prepared by the dilution of analytical grade hydrochloric acid (37%) with double distilled water and all the experiments were carried out in the unstirred solutions.

The weight loss study was carried out on mild steel strips of 5.0cm x 2.0cm x 0.025cm dimension. The electrochemical measurements were carried out on mild steel strips with the dimension 1.0cm x 1.0cm exposed with a 7.5 cm long stem (coated by the commercially available lacquer).

2.3. Weight loss measurements

Weight loss or gravimetric measurements were performed on mild steel sample by immersing it

in the absence and presence of different concentrations of PDA at308Kf or 3h duration in 1M HCl solution. The inhibition efficiency (%) was determined using the following equation:

$$\eta_{WL} = \frac{W_o - W_i}{W_o} \times 100 \quad (1)$$

where W_o and W_i are the weight loss values in absence and presence of inhibitor. The weight loss measurements were also carried out at different time intervals, different concentrations of the acid solution and at different temperatures.

2.4. Potentiodynamic polarization

The electrochemical behaviour of mild steel sample in inhibited and non-inhibited solution was studied by recording anodic and cathodic potentiodynamic polarization curves. Measurements were performed in the 1M HCl solution containing different concentrations of the tested inhibitor by changing the electrode potential automatically from −250 to +250mV versus corrosion potential at a scan rate of 1mVs^{-1}. The linear Tafel segments of anodic and cathodic curves were extrapolated to corrosion potential to obtain corrosion current densities (I_{corr}).

The inhibition efficiency was evaluated from the measured I_{corr} values using the following relationship:

$$\eta_{TP} = \frac{I^o_{corr} - I^i_{corr}}{I^o_{corr}} \times 100 \quad (2)$$

where, I^o_{corr} and I^i_{corr} are the corrosion current densities in the absence and presence of inhibitor, respectively.

2.5. Linear polarization measurement

The linear polarization study were carried out from cathodic potential of -0.02V *vs.* OCP to an anodic potential of +0.02V vs OCP at a sweep rate 0.125 mVs^{-1} to study the polarization resistance ($R_{p)}$ in 1 M HCl solution with and without different concentration of inhibitor. Polarization resistance (R_p) was evaluated from the slope of the curve in the vicinity of the corrosion potential. The inhibition efficiency was calculated from the polarization resistance values by the relationship as follows:

$$\eta_{Rp} = \frac{\left(1/R^o_p\right) - \left(1/R^i_p\right)}{\left(1/R^o_p\right)} \times 100 \quad (3)$$

where, R^o_p and R^i_p are the polarization resistance in absence and presence of inhibitor, respectively.

2.6. Electrochemical impedance spectroscopy

The EIS tests were performed at 308±1K in a three electrode assembly. A saturated calomel electrode was used as a reference and a 1 cm^2 platinum foil was used as counter electrode. All the potentials were measured versus SCE. The electrochemical impedance spectroscopy measurements were perform using a Gamry instrument potentiostat / galvanostat with a Gamry framework system based on ESA 400 in a frequency range 10^{-2}Hz – 10^5 Hz under potentiodynamic conditions with amplitude of 10 mV peak to peak, using AC signal at E_{corr}. Gamry applications include software DC105 for corrosion and EIS300 for EIS measurements and Echem analyst version 5.50 software packages for data fitting. The experiments were carried out after 30 minutes of immersion in the test solution without deaeration and stirring.

The inhibition efficiency of the inhibitor was calculated from the charge transfer resistance values using following equation:

$$\eta_{Rt} = \frac{\left(1/R_t^o\right) - \left(1/R_t^i\right)}{\left(1/R_t^o\right)} \times 100 \quad (4)$$

where, R_t^o and R_t^i are the charge transfer resistances in the absence and in presence of inhibitor respectively.

3. RESULTS AND DISCUSSIONS

3.1. Weight loss method

3.1.1. Effect of inhibitor concentration

Weight loss measurements were carried out for the different concentrations of inhibitor. The weight loss, inhibition efficiency and corrosion rate were reported in the Table1. The trend of the inhibition efficiency with respect to the PDA concentration was plotted in Figure 1(A) to show the trend of increment of the inhibition efficiency. It is evident from the Table 1 that the corrosion rate decreases and the inhibition efficiency increases with increase in the PDA concentration.

3.1.2. Effect of Immersion time

Effect of the immersion versus inhibition efficiency graph was plotted in the figure 1(b). It is clear from the Figure 1(B) that the increase in the immersion time does not affect much on the inhibition efficiency, although the inhibition efficiency decreases with increase in the immersion time with very slow rate.

This very slow decrease in inhibition efficiency suggesting that the compound is very firmly adsorbed on the mild steel surface and desorption rate is very slow.

3.2.3. Effect of acid concentration

Increase in the acid concentration with respect to the inhibition efficiency is reported in the figure 1(C). It is evident from the figure 3 that the inhibition efficiency decreases with very slow rate, suggested that the compound is very effective at higher concentration of the acid solution.

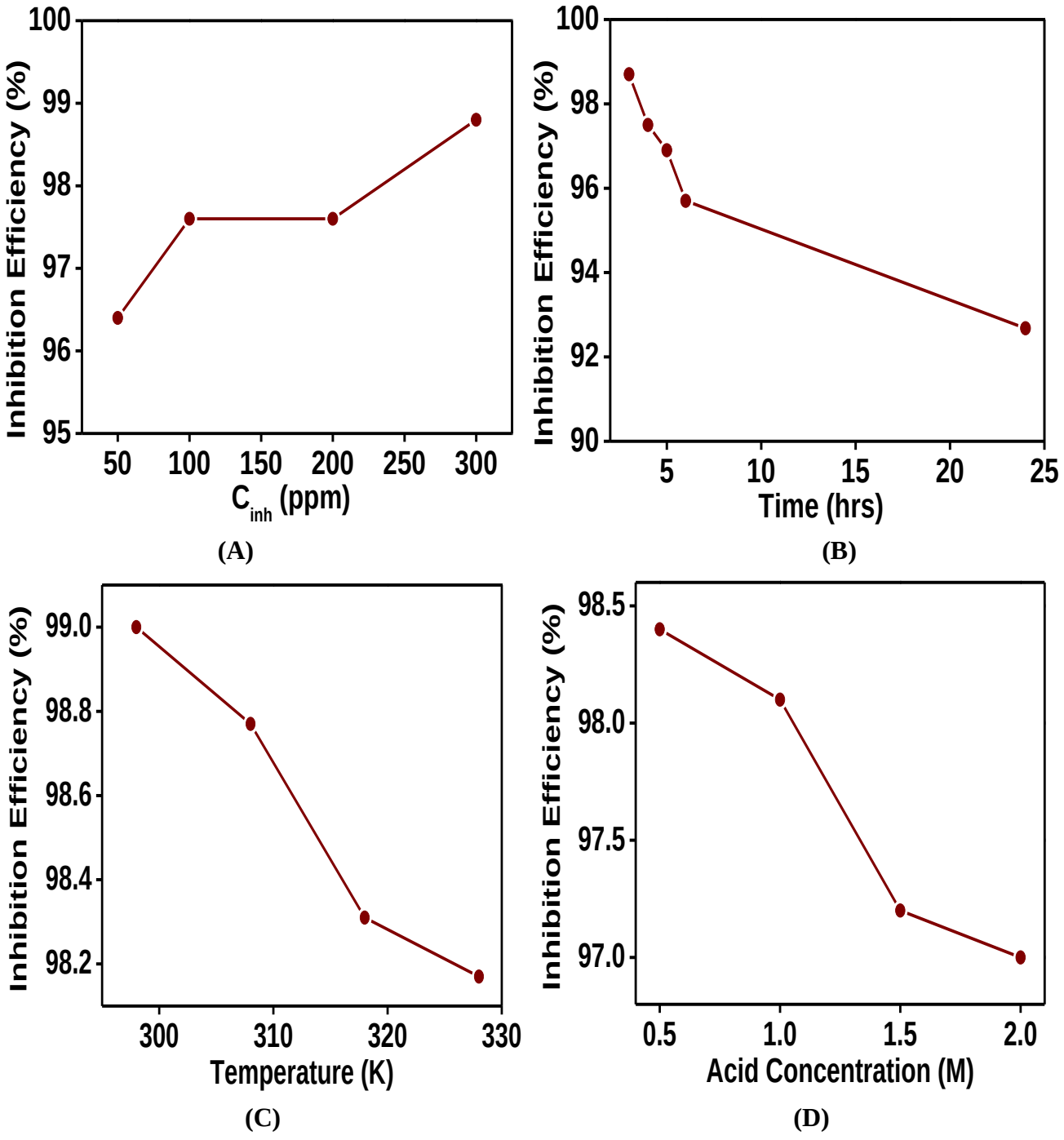

Figure 1. Variation of inhibition efficiency in 1M HCl on mild steel of surface area 20 cm^2 with (A) different concentration of inhibitor (B) different immersion time (C) different acid concentration and (D) different temperature range; using weight loss data.

3.1.4. Effect of temperature

Effect of the temperature was studied with the optimum concentration of the PDA at the range of 298-328K. Influence of temperature on the inhibition efficiency shown in Figure 1(D). It is observe that the inhibition efficiency almost steady with increase in the solution temperature. The negligible change in inhibition efficiency with temperature may attribute to the strong adsorption of the inhibitor molecule from metal surface.

3.1.5. Adsorption isotherm

Adsorption isotherm study describes the adsorptive behaviour of organic inhibitors to know the adsorption mechanism. The most usually used adsorption isotherms are Langmuir, Temkin, Frumkin and other various isotherms. The surface coverage (θ) values were calculated using weight loss data.

Langmuir adsorption isotherm were tested and found most appropriate isotherm to explain the experimental data. Langmuir adsorption isotherm is represented by following equations:

$$\frac{C_{inh}}{\theta} = \frac{1}{K_{ads}} + C_{inh} \qquad (5)$$

where, K_{ads} is the adsorption equilibrium constant and C_{inh} is the concentration of inhibitor used in the corrosive medium. A straight line was obtained by plotting the graph of C_{inh} vs C_{inh}/θ with the R value almost unity (0.9999) (Figure 2). The slope is reported almost unity suggesting that the Langmuir adsorption isotherm model provides the best description of the adsorption behaviour.

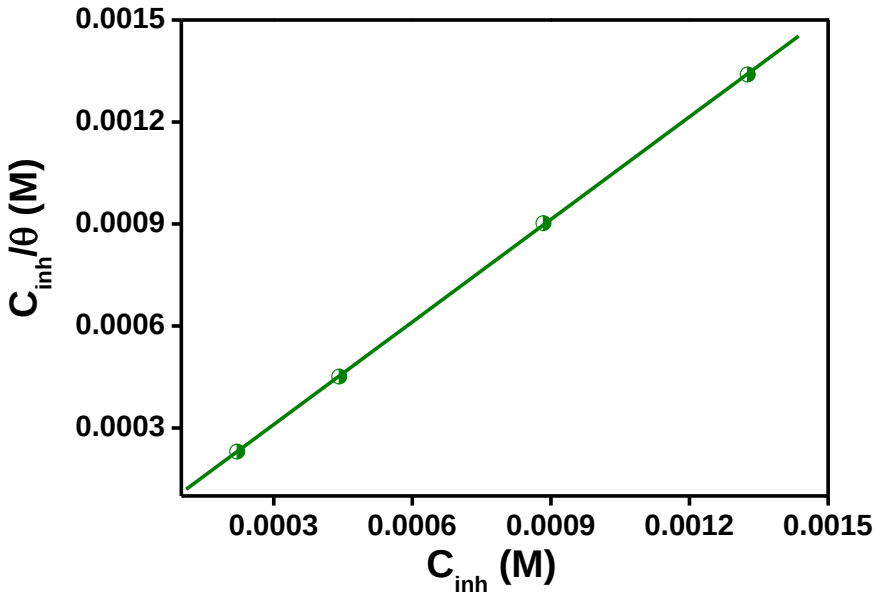

Figure 2. Langmuir's Adsorption isotherm plot for the adsorption of PDA in 1MHCl on the surface of mild steel

Table 1. Calculated parameters for Langmuir adsorption isotherm for mild steel in 1 M HCl in absence and presence of PDA at 308K.

Temperature (K)	K_{ads} (mol^{-1})	Slope	R^2	$-\Delta G_{ads}$ (kJ mol^{-1})
308	1.2×10^5	1.0050	0.9999	40.20

3.1.6. Kinetic and thermodynamic consideration

It is well known that the logarithm of the corrosion rate is a linear function with 1/T (Arrhenius equation) [18-20]:

$$\log C_R = \frac{-E_a}{2.303RT} + \log \lambda \qquad (6)$$

where, E_a is the apparent activation energy, R molar gas costant and λ the Arrhenius pre exponential factor.

A plot shown in Figure 3 (A), of corrosion rate obtained by weight loss measurement versus 1/T gave straight line. The value of the E_a obtained from the slope equals to the ($-E_a$ / 2.303R) and the pre exponential factor calculates by the intercept (logλ) of the line reported in Table 2. It is evident from the Table 2 that the activation energy increased on addition of PDA in comparison to the uninhibited solution. The increase in the apparent activation energy value interpreted as the decrease in the inhibition efficiency with the increase in the temperature. This leads to the increase in corrosion rate due to the greater area of metal that is exposed towards the corrosive environment [21].

The dependence of corrosion rate on temperature can also be expressed using the transition state equation. An alternative formula for the Arrhenius equation is the transition state equation [22]:

$$C_R = \frac{RT}{NH}\exp\left(\frac{\Delta S^*}{R}\right)\exp\left(-\frac{\Delta H^*}{RT}\right) \qquad (7)$$

where, h is Plank's constant, N the Avogadro's number, ΔS^* the apparent entropy of activation and $\Delta H^*$the enthalpy of activation. A plot of log (C_R/T) versus 1/T is shown in Figure 3 (B). Straight lines were obtained with slope ($-\Delta H^*$/2.303R) and intercept of [log(R/Nh) + (ΔS^*/2.303R)], from which ΔH^* and ΔS^*were calculated and listed in Table 2. It is clear from the Table 2 that the entropy of activation increased in the presence of inhibitor in comparison to the uninhibited sample. The increase in the activation entropy in presence of inhibitor indicates the increase in the disorderliness on going from reactant to activated complex. It is evident from the table that the value of ΔH^* increased in the presence of inhibitor than in the uninhibited solution indicating the higher inhibitive efficiency. This may be attributed to the presence of an energy barrier for the reaction, hence, the process of adsorption of inhibitor leads to rise in enthalpy of the corrosion process.

The heat of adsorption (ΔQ_{ads}) was obtained from the surface coverage and temperature by using following equation:

$$\log\left(\frac{\theta}{1-\theta}\right) = \log A + \log C_{inh} - \left(\frac{\Delta Q_{ads}}{2.303RT}\right) \quad (8)$$

A plot of log(θ/1-θ) vs 1/T is given in Figure 3(C). The value of heat of adsorption was determined from the slope ($-\Delta Q_{ads}/2.303R$) of the graph. The value of heat of adsorption is given in Table 2. It is evident from the Table 2 that ΔQ_{ads} has negative value which indicates that inhibitor adsorption decreases with increase in the temperature hence decrease in inhibitor efficiency [23]. The negative value of ΔQ_{ads} also suggested that the adsorption of inhibitor is an exothermic process [24].

Free energy of adsorption (ΔG_{ads}) was calculated using the following equations [25]:

$$K_{ads} = \frac{1}{55.5}\exp\left[\frac{-\Delta G^{o}_{ads}}{RT}\right] \quad (9)$$

This equation can also be express in the form as follows:

$$\Delta G_{ads} = -2.303RT\log(55.5K_{ads}) \quad (10)$$

where, ΔG_{ads} is Gibbs free energy of adsorption, T is the temperature in Kelvin and K_{ads} is the equilibrium constant for the adsorption process and 55.5 is the molar concentration of water in solution. K_{ads} value was calculated from the intercept of the Figure 2 and presented in Table 1.

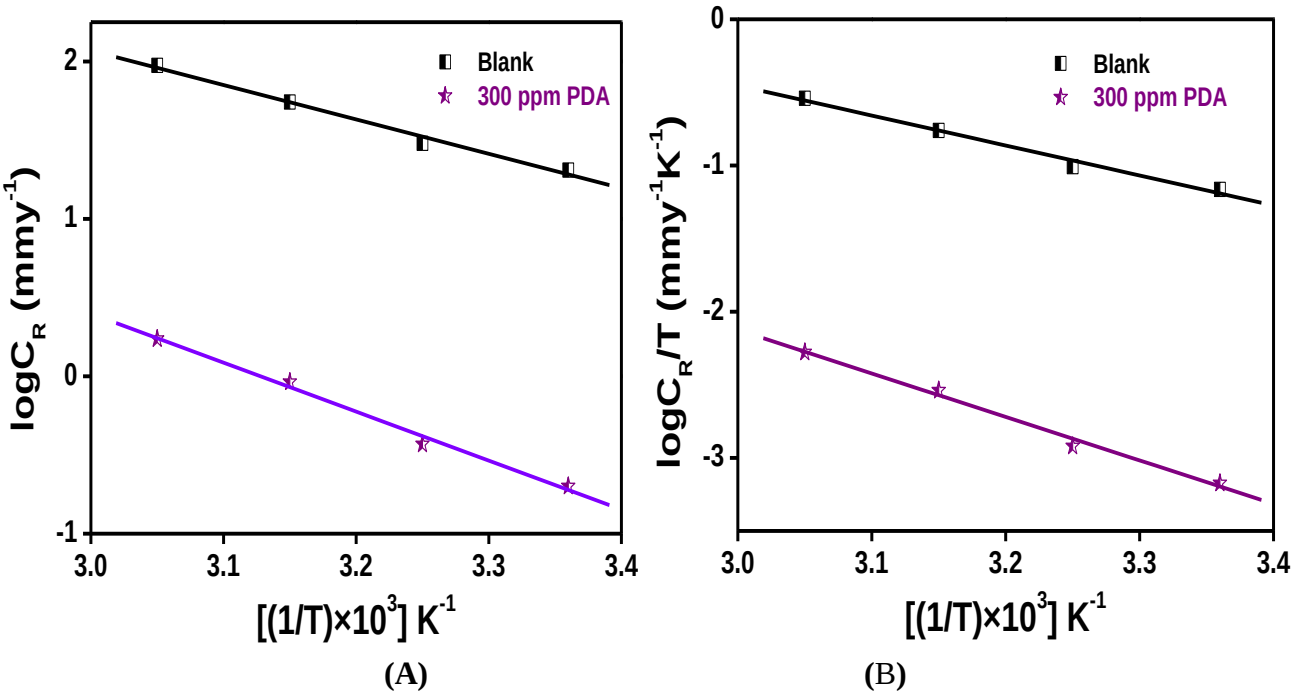

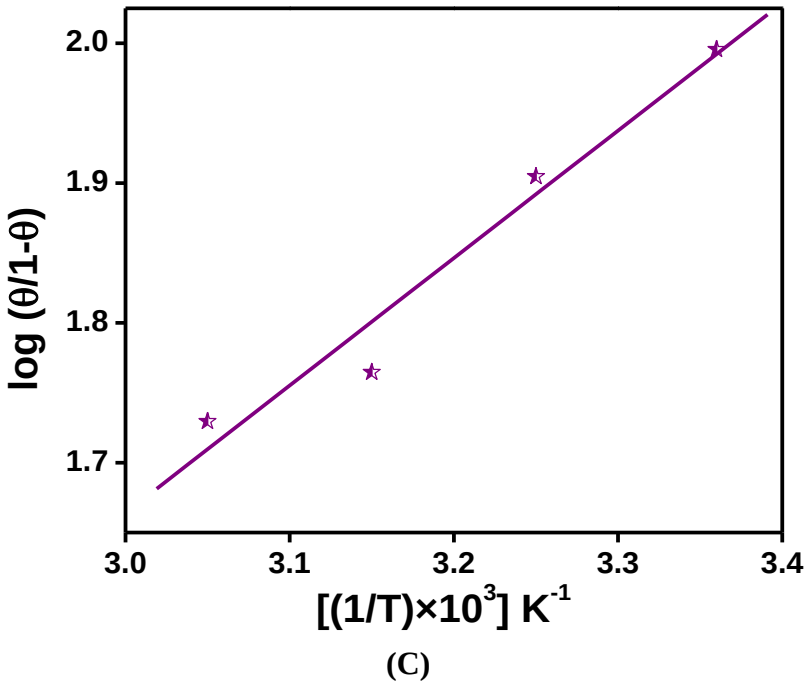

Figure 3. Adsorption isotherm plots in absence and presence of PDA inhibitor in 1M HCl solution (A) *log* (C_R) versus *1/T* (B) log (C_R/T) versus *1/T* (C) ($\theta/1-\theta$) versus *1/T*

ΔG_{ads} values calculated using eq.10 is presented in Table 1. The negative value of Gibbs free energy ensures the spontaneity of adsorption process and stability of the adsorbed layer on the surface of mild steel.

Table 2. Thermodynamic parameters for mild steel in 1M HCl in absence and presence of PDA.

Inhibitor Concentration	E_a (kJ mol^{-1})	λ (mg cm^{-2})	ΔH^* (kJ mol^{-1})	ΔS^* (J mol^{-1} K^{-1})	ΔQ_{ads} (kJ mol^{-1})
Blank	41.74	4.2×10^{8}	39.26	-88.43	-
300 ppm PDA	59.55	5.3×10^{9}	56.94	-67.38	17.46

3.2. Linear Polarization measurement:

Polarization resistance (R_p) values were determined from the slope of the potential current lines [26]:

$$R_p = A\frac{dE}{dI} \qquad (11)$$

where A is the surface area of the electrode, dE is change in potential and dI is change in current. The inhibition efficiency and polarization resistance parameters are listed in Table 3. It is

evident from the Table 3 that inhibition efficiency increases with increase in the polarization resistance and polarization resistance value increases with the inhibitor in comparison to the blank.

3.3. Potentiodynamic polarization:

The potentiodynamic polarization measurements were carried out to study the kinetics of the cathodic and anodic reactions. Figure 4 shows the results of the effect of PDA inhibitor on the cathodic as well as anodic polarization curves of mild steel in 1M HCl respectively. It is evident from the figure that both reactions were suppressed with the addition of the inhibitor. This suggests that PDA reduced the anodic dissolution reactions as well as retarded the hydrogen evolution reactions on the cathodic sites.

Electrochemical corrosion kinetic parameters namely corrosion potential (E_{corr}) and corrosion current density (I_{corr}) obtained from the extrapolation of the polarization curves are listed in Table 3. The corrosion current density (I_{corr}) decreased by the increase in the adsorption of the inhibitor with increasing inhibitor concentration. The inhibition efficiency increases with increase in the inhibitor concentration was calculated by the I_{corr} values and listed in Table 3.According to Ferreira et.al [27] and Li et. al. [28], if the displacement in corrosion potential is more than 85 mV with respect to the corrosion potential of blank solution, the inhibitor can be consider as a cathodic or anodic type. In present study, displacement was 14 mV with respect to the corrosion potential of the uninhibited sample which indicates that the studied inhibitor is a mixed type of inhibitor. The results obtained from Tafel polarization showed good agreement with the results obtained from the linear polarization resistance.

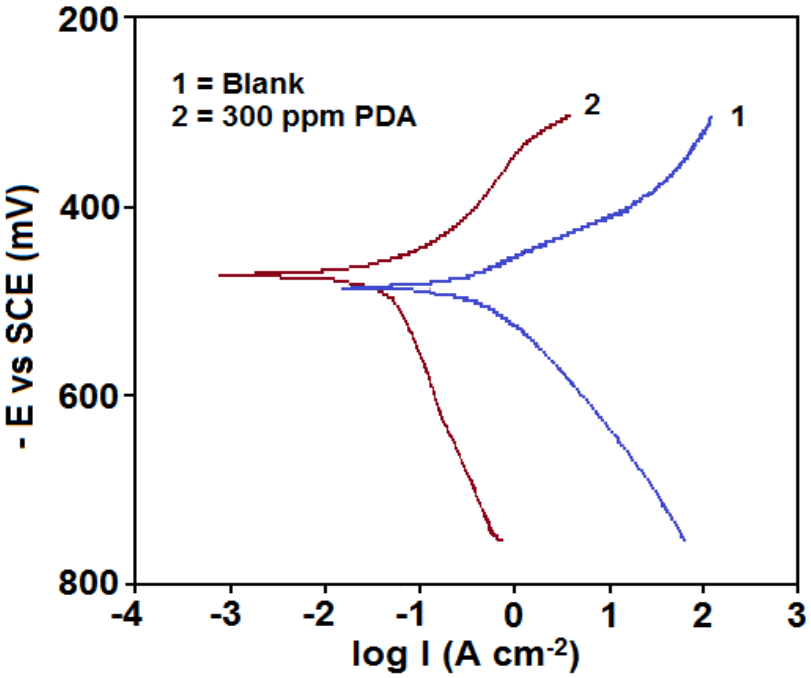

Figure 4. Potentiodynamic polarization curves for the corrosion of mild steel in 1N HCl without and with 300 ppm PDA

3.4. Electrochemical impedance spectroscopy:

Nyquist representation of the EIS study of mild steel in 1M HCl in absence and presence of 300 ppm PDA were presented in figure 5. The large capacitive loop attributed to the adsorption of the inhibitor molecule [29]. The simple equivalent Randle circuit for studies is shown in Fig. 6, where R_s represents the solution and corrosion product film; the parallel combination of resister, R_t and capacitor C_{dl} represents the corroding interface. The existence of single semi circle showed the single charge transfer process. Depression from the perfect semi circle is due to the inhomogeneous nature of the metal surface arising from the surface roughness or the interfacial phenomenon [30]. The increase in R_t value due to the addition of inhibitor in comparison to the absence of inhibitor is attributed to the formation of protective film on the metal/solution interface. These observations suggest that PDA molecules function by adsorption at metal surface thereby causing the decrease in C_{dl} values and increase in R_t values [29-31]. The charge transfer resistance (R_t) and the interfacial double layer capacitance (C_{dl}) derived from these curves are given in Table 3. Inhibition efficiency was calculated by the using the charge transfer resistance values. The results obtained from the EIS studies showed good agreement with the results obtained from the Tafel polarization.

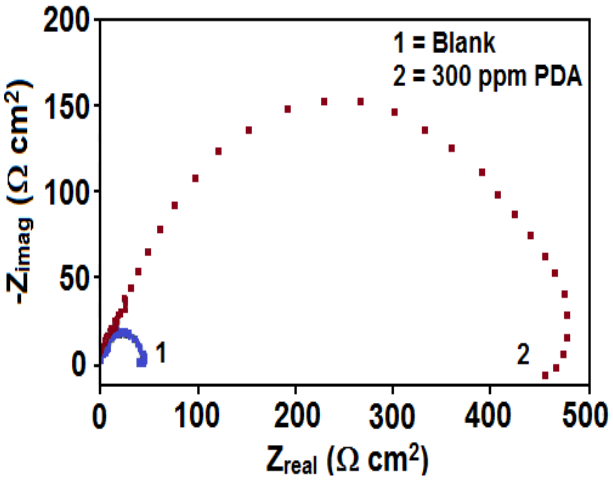

Figure 5. Nyquest plot for mild steel corrosion in absence and presence of 300 ppm PDA.

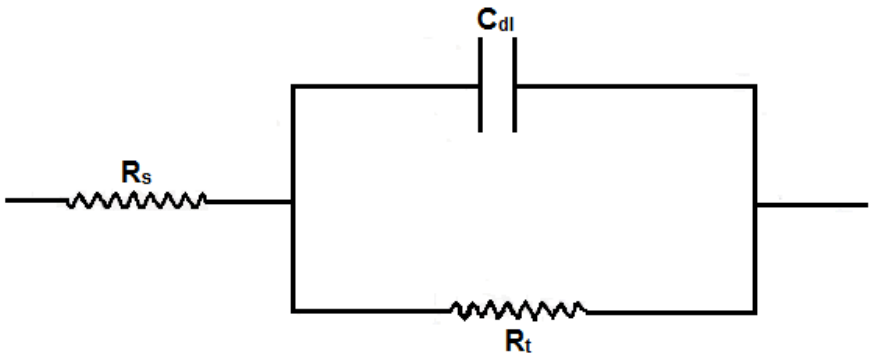

Figure 6. The electrochemical equivalent circuit used to fit the impedance measurements.

Table 3. Electrochemical parameters for the corrosion of mild steel 1 M HCl in absence and presence of PDA.

Electrochemical Techniques	Parameters	Blank	300 ppm PDA
Polarization Resistance	R_p (Ω Cm^2)	16.1	561.0
	η_{Rp} (%)	-	97.1
Tafel Polarization	E_{corr} (mV vs SCE)	-485.0	-472.0
	I_{corr} (μA cm^{-2})	455.0	62.2
	η_{TP} (%)	-	86.3
Electrochemical Impedance Spectroscopy (EIS)	R_t (Ω Cm^2)	41.3	461.3
	C_{dl} ($mFCm^{-2)}$	24.2	2.17
	η_{Rt} (%)	-	91.0

3.4. Mechanism of Inhibition

Corrosion inhibition of mild steel in 1M HCl by PDA can be explained on the basis of molecular adsorption of inhibitor on to the metal surface. It is generally considered that the first step in the corrosion inhibition of a metal is the adsorption of the inhibitor molecules at metal / solution interface [32]. Organic compounds are adsorbed on the metal surface by (a) electrostatic interaction between the charged molecules and charged metal; (b) interaction of π-electrons with the metal; (c) interaction of unshared pair of electrons in the molecule with the metal; and (d) the combination of the all the effects [33,34].

4. CONCLUSIONS

All the measurements showed that the PDA has excellent inhibition properties against the mild steel corrosion in hydrochloric acid solution. EIS measurements also indicates that the inhibitor performance increase due to the adsorption of molecule on the metal surface. Potentiodynamic polarization measurements showed that the inhibitor acts as mixed type of inhibitor. The inhibitor showed maximum inhibition efficiency at 300 ppm concentration of the studied inhibitor. The inhibition efficiencies determined by EIS, potentiodynamic polarization and weight loss studies are in good agreement. The inhibitor follows the Langmuir adsorption isotherm in the process of adsorption. Thermodynamic calculations show that the adsorption process is spontaneous, exothermic in nature.

ACKNOWLEDGEMENTS
SKS and AKS acknowledge the North West University for a Postdoctoral Fellowship.

References

1. S.K. Shukla, M.A. Quraishi, E.E. Ebenso, *Int. J. Electrochem. Sci.* 6 (2011) 2912.
2. S.K. Shukla, M.A. Quraishi, *Corros. Sci.* 51 (2009) 1007.

3. A.K. Singh, S.K. Shukla, M. Singh, M.A. Quraishi, *Mater. Chem. Phys.* 129 (2011) 68.
4. S.K. Shukla, A.K. Singh, I. Ahmad, M.A. Quraishi, *Matter. Lett.* 63 (2009) 819.
5. S.A. Umoren, I.B. Obot, E.E. Ebenso, *E-Journal Chem.* 5 (2008) 355.
6. S.K. Shukla, M.A. Quraishi, R. Prakash, *Corros. Sci.* 50 (2008) 2867.
7. F. Bentiss, M. Bouanis, B. Mernari, M. Traisnel, M. Lagrenee, *J. Appl. Electrochem.* 32 (2002) 671.
8. F. Bentiss, M. Traisnel, M. Langrenee. *Corros. Sci.* 42 (2000) 127.
9. M.A. Quraishi, S.K. Shukla, *Mater. Chem. Phys.* 113 (2009) 685.
10. M. Langrenee, B. Mernari, N. Chaibi, M. Traisnel, H. Vezin, F. Bentiss, *Corros. Sci.* 43 (2001) 951.
11. M. El-Azhar, B. Mernari, M. Traisnel, F. Bentiss, M. Lagrenee, *Corros. Sci.* 43 (2001) 2229.
12. M.A. Ameer, E. Khamis, G. Al-senani, *J. Appl. Electrochem.* 32 (2002) 149.
13. E.E. Ebenso, *Mater. Chem. Phys.* 79 (2003) 58.
14. H.L. Wang, H.B. Fan, J.S. Zhang. *Mater.Chem.Phys.* 77 (2002) 655.
15. X.H. To, N. Pebere, N. Pelaprat, B. Boutevin, Y. Hervaud, *Corros. Sci.* 39 (1997) 1925.
16. K. Aramaki, T. Kiuchi, T. Sumiyoschi, H. Nishihara, *Corros. Sci.* 32 (1991) 593.
17. A.P. Singh, R. Singh, V.K. Verma, *Heterocycles* 27 (1988) 10.
18. M. Schorr, J. Yahalom, *Corros. Sci.* 12 (1972) 867.
19. S.A. Umoren, M.M. Solomen, I.I. Udousoro, A.P. Udoh, *Corros. Sci.* 52 (2010) 1317.
20. M.G.A. Khedr, A.M.S. Lashien, *Corros. Sci.* 33 (1992) 137.
21. T. Szauer, A. Brandt, *Electrochim Acta* 26 (1981) 1253.
22. S.S.A. Rehim, H.H. Hassan, A.A. Mohammed, *Mater. Chem. Phys.*, 70 (2001) 64.
23. H.M. Bhajiwala, R.T. Vashi, *Bull. Electrochem.* 17 (2001) 441.
24. X.H. Li, G.N. Mu, *Appl. Surf. Sci.* 252 (2005) 1254.
25. M. Schorr, J. Yahalom, *Corros. Sci*, 12 (1972) 867.
26. A.K. Singh, M.A. Quraishi, *J. Appl. Electrochem.* 41 (2011) 7.
27. E.S. Ferreira, C. Giancomelli, F.C. Giacomelli, A. Spinelli, *Mater. Chem. Phys.* 83 (2004) 129.
28. W.H. Li, Q. He, C.L. Pei, B.R. Hou, *J. Appl. Electrochem*. 38 (2008) 289.
29. S.K. Shukla, M.A. Quraishi, *Corros. Sci.* 52 (2010) 314.
30. S.K. Shukla, M.A. Quraishi, *Corros. Sci* 51 (2009) 1990.
31. F. Bentiss, M. Traisnel, M. Lagrenee, *Corros. Sci.* 42 (2000) 127.
32. M. Sahin, S. Bilgic, H. Yilmaz, *Appl. Surf. Sci.*195 (2002) 1.
33. H. Shorky, M. Yuasa, I. Sekine, R.M. Issa, H.Y. El-Baradie, G.K. Gomma, *Corros. Sci.* 40 (1998) 2173.
34. D.P. Schweinsberg, G.A. George, A.K. Nanayakkara, D.A. Steiner, *Corros. Sci.* 28 (1988) 33.